Strojniški vestnik - Journal of Mechanical Engineering 54(2008)1, 3-10
UDC 627.84
Paper received: 4.10.2006
Paper accepted: 19.12.2007

Analysis of Hydraulic Characteristics of Guard-Gate for Hydropower Plant

Zlatko Rek[1,*] - Anton Bergant[2] - Miha Röthl - Primož Rodič[3] - Iztok Žun[1]
[1]University of Ljubljana, Faculty of Mechanical Engineering, Slovenia
[2]Litostroj E.I., Slovenia
[3]Institute of Hydraulic Research, Slovenia

A guard-gate can be installed at the inlet of the pressure tunnel, at the downstream end of the surge tank or in the draft tube of the water turbine. A hydraulic shape of the gate and characteristics of the hydropower plant flow-passage sytem govern the magnitude of pressure forces acting on the gate structure. Flow conditions at the downstream end of the gate may require adequate air admission. Numerical analysis of hydraulic characteristics has been performed for a vertical leaf gate at different gate openings. The analysis has been performed with Computational Fluid Dynamics (CFD) code using finite volume method. Computational results are compared with results of measurements carried out in a model test rig.

Keywords: hydropower plant, guard-gates, hydraulic characteristics, control volume methods

0 INTRODUCTION

The guard-gate can be installed at the inlet of the pressure tunnel, at the downstream end of the surge tank or in the draft tube of the water turbine [1], Figure 1. A hydraulic shape of the gate and characteristics of the flow-passage system of the power plant govern the magnitude of pressure forces during the gate closure. Early experimental investigations of the hydrodynamic behaviour of gates have been carried out in the sixties [2] and [3]. Two types of flow at the downstream end of the gate have been observed: pressurized flow and free surface flow. Flow conditions at the downstream end of the gate may induce very low pressures; there is increased danger of pipeline collapse and large pressure oscillations. Air admission at the downstream end of the gate

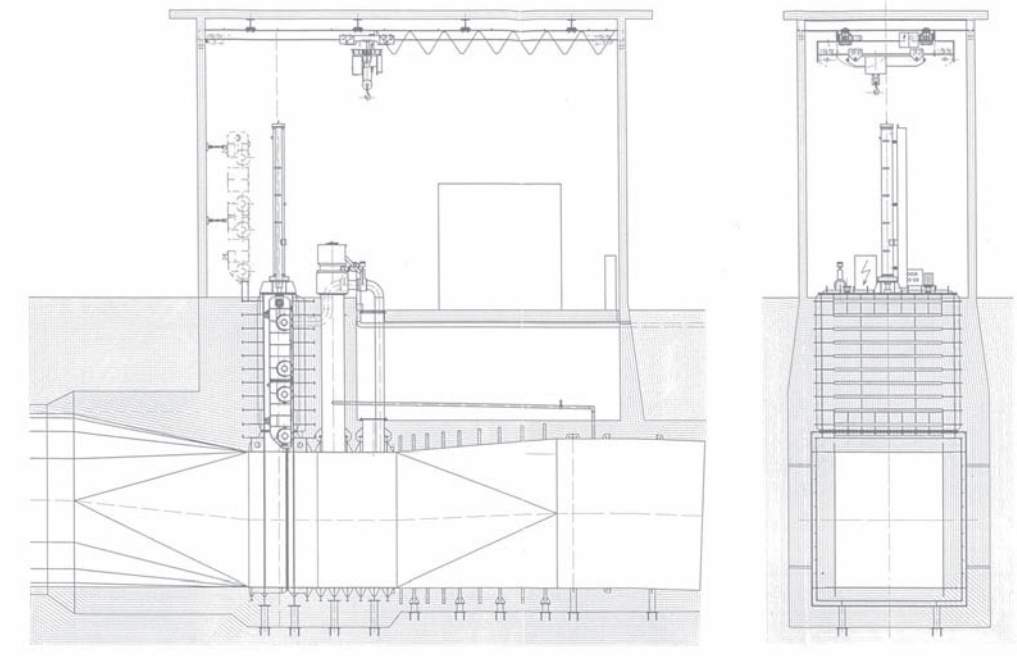

Fig. 1. Guard-gate

*Corr. Author's Address: University of Ljubljana, Faculty of Mechanical Engineering, Aškerčeva 6, SI-1000 Ljubljana, Slovenia, zlatko.rek@fs.uni-lj.si

attenuates pressure oscillations [4]. Hydraulic forces acting on the gate structure have been carefully investigated [5] and [6]. The magnitude of hydraulic forces is needed for design of the gate body and hoist mechanism.

The paper deals with numerical flow investigations of a vertical guard-gate at different gate openings. Flow computations are performed by standard numerical methods [7]. A three-dimensional finite volume method (FVM) is used [8] and [9]. The FVM is a direct method i.e. the geometry of the gate should be defined in advance. The computational results are compared with results of measurements in a hydraulically similar gate. The measurements were performed at the Institute of Hydraulic Research in Ljubljana. Validation study includes comparison of flow characteristics i.e. pressure on the gate structure. The accuracy and robustness of the numerical model (selection of appropriate turbulence model) are tested for a number of operating regimes and conclusions about industrial application of the model are drawn. This would reduce costs for future laboratory testing. Hydraulic characteristics of the gate are essential for optimum design of the gate (body, areation pipe, hoist mechanism) and prediction of operating regimes in the hydropower plant flow-passage system [6].

1 COMPUTATIONAL MODEL

Water flow through channel with guard-gate at fixed opening is cosidered as steady-state flow of viscous incompressible fluid. Flow is turbulent (Re = 174 000) due to the large volume flowrate (Q = 44.7 l/s) and pipe diameter (D = 0.32 m). RANS (Reynolds Averaged Navier-Stokes) k-ε turbulent model with wall functions [10] was used. Despite of some deficencies, this model is known to be the most applicable turbulent model for solving real engineering problems [11].

1.1 Governing equations

Water flow is governed by conservation laws [10] and [12] for:

mass

$$\frac{\partial \rho}{\partial t} + \nabla \cdot (\rho \mathbf{U}) = 0 \tag{1}$$

momentum

$$\frac{\partial}{\partial t}(\rho \mathbf{U}) + \nabla \cdot (\rho \mathbf{U} \otimes \mathbf{U}) = -\nabla p + \nabla \cdot \left(\mu_{ef} \left(\nabla \mathbf{U} + (\nabla \mathbf{U})^T\right)\right) - \rho \mathbf{g} \tag{2}$$

turbulent kinetic energy (t.k.e.)

$$\frac{\partial}{\partial t}(\rho k) + \nabla \cdot (\rho \mathbf{U} k) = \nabla \cdot \left(\left(\mu + \frac{\mu_t}{\sigma_k}\right) \nabla k\right) + \mu_{ef} \nabla \mathbf{U} \cdot \left(\nabla \mathbf{U} + (\nabla \mathbf{U})^T\right) - \rho \varepsilon \tag{3}$$

and dissipation of t.k.e.

$$\frac{\partial}{\partial t}(\rho \varepsilon) + \nabla \cdot (\rho \mathbf{U} \varepsilon) = \nabla \cdot \left(\left(\mu + \frac{\mu_t}{\sigma_\varepsilon}\right) \nabla \varepsilon\right) + C_1 \frac{\varepsilon}{k} \left(\mu_{ef} \nabla \mathbf{U} \cdot \left(\nabla \mathbf{U} + (\nabla \mathbf{U})^T\right)\right) - C_2 \rho \frac{\varepsilon^2}{k} \tag{4},$$

where: ρ – density, μ – dynamic (laminar) viscosity, $\mu_t = C_\mu \rho k^2/\varepsilon$ – turbulent viscosity, $\mu_{ef} = \mu + \mu_t$ – effective viscosity, $\boldsymbol{g}$ – gravity acceleration, $\mathbf{U}$ – time averaged velocity vector, k – turbulent kinetic energy, ε – dissipation of turbulent kinetic energy. Constants of turbulent model are represented in Table 1.

Table 1. *Constants of turbulent model*

C_μ	C_1	C_2	σ_k	σ_ε
0.09	1.44	1.92	1.00	1.22

1.2 Discrete model

Geometric model, Figure 2, was built with CFX-build pre-processor. Because CFX solver uses blok-structured grids, the model is composed by 72 blocks (solids). Three different geometries were considered: 30%, 70% and 100% openings.

Grid density is very important in the numerical solution [13]. If it is too coarse (large control volumes)

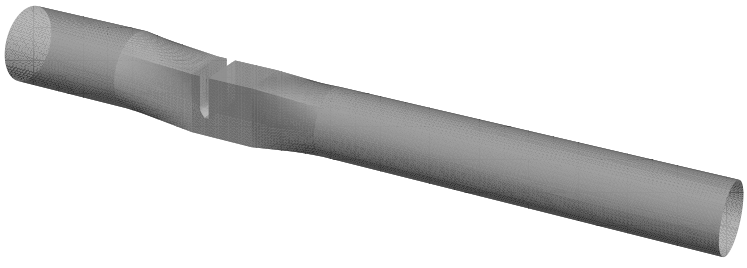

Fig. 2. *Geometric model of guard-gate at 30% opening*

the solution wil not be accurate enough or iterations will not converge at all. For very fine grid (small control volumes) there is a drastically increase in computational time, computer memory and disk space. So, the compromising grid size has to be found. In our case, the grid dependency study [9] is performed on the model with 30% opening for three grid densities:

- coarse, Figure 3,
- medium, Figure 4,
- fine, Figure 5.

The upstream end of the guard-gate was selected for analysis of pressure profile results because the flow conditions are most interesting there. We can see from Figure 6 that results for coarse grid exceedingly deviate and therefore this grid is not appropriate for numerical analysis. Much better

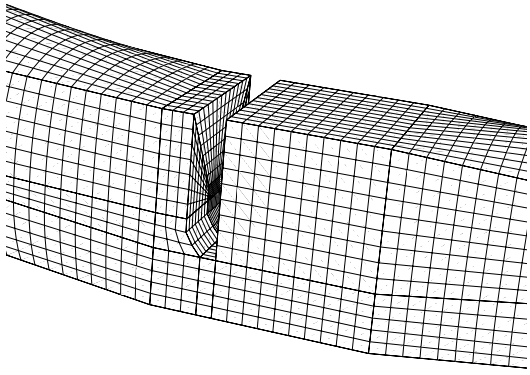

Fig. 4. *Medium grid, 86615 control volumes*

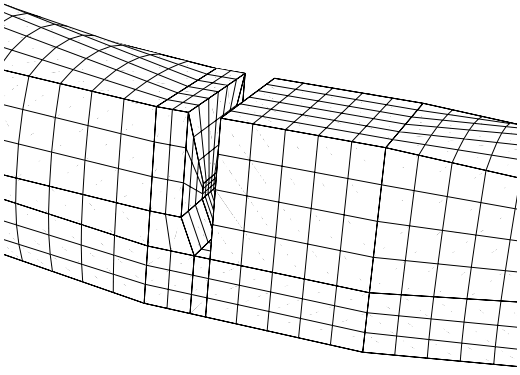

Fig. 3. *Coarse grid, 9294 control volumes*

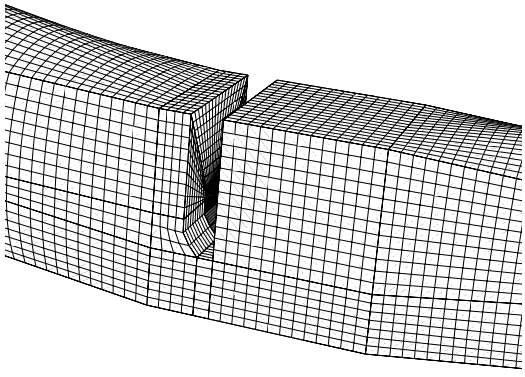

Fig. 5. *Fine grid, 197511 control volumes*

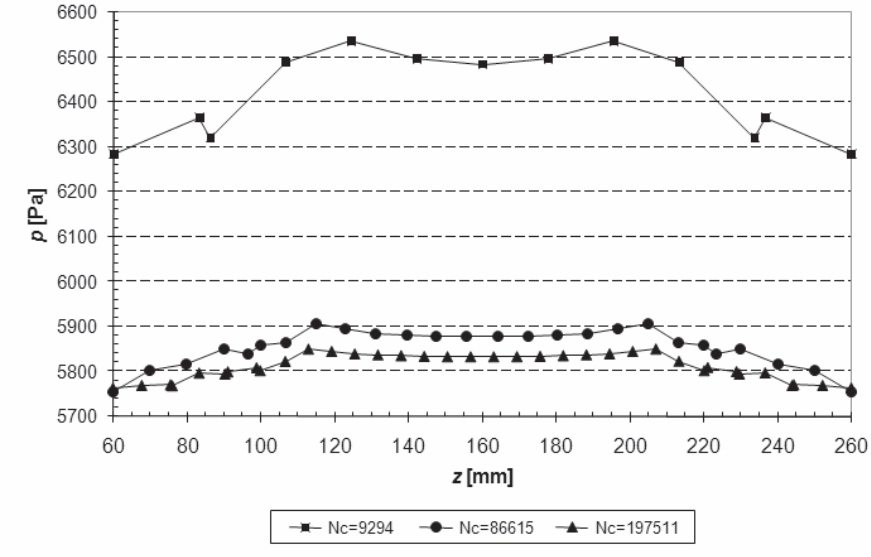

Fig. 6. *Computational grid dependency test*

agreement is with medium and fine grid. Values for pressure on the wall are practically the same. Due to the computer limitations (CPU time, available memory and disk space) and fact that we will compare values for pressure on the wall, we used the medium grid for the rest of the geometry models. We also checked criteria for grid quality, such as: Orthogonal Deviation, Grid Expansion, Skew Ratio and Twist Angle. All parameters were within recommended value intervals [10].

Velocity U = 0.56 m/s (volume flowrate Q = 44.7 l/s), 5% turbulence intensity and turbulence length scale l_{Σ} = 0.01 m were prescribed as inlet boundary condition. Numerical model doesn't include the whole geometry, because the computational domain extends to the measuring point P14; we use measured values for pressure as outlet boundary condition, Table 2.

Table 2. *Boundary conditions at outlet*

Opening [%]	p [Pa]
30	3154
70	9224
100	9221

Initial condition for velocity was **U** = (0.56 m/s, 0, 0).

1.3 Computation

The commercial CFD package CFX-4.4 from ANSYS was used for flow analysis. The discretized domain and command file with control parameters and material properties are needed to solve the system of equations. Density and dynamic viscosity at 20°C were 997.8 kg/m^3 and 0.00102 kg/ms respectively.

The code uses a segregated solver. This means that a linearized system of transport equations is solved for each variable *U, V, W, k* and *ε*. The pressure-implicite with splitting of operators (PISO) correction scheme was used for pressure computation. To solve the system of linear equations for velocity, a Block Stone (BLST) linear solver was used. For pressure, a method of Conjugate Gradients (ICCG) and for turbulence, a Line Relaxation (LRLX) method were used. Reduction factors were: 0.1 for pressure and 0.25 for velocity and turbulence. The velocity field and turbulence quantities were discretized with a upwind differencing scheme (UDS), while pressure field was discretized with a central difference scheme (CDS). Under-relaxation factors were: 0.5 for velocity, 0.8 for turbulence and 1.0 for pressure. Convergence criteria residual mass flow was 10^{-5} kg/s. Figure 7 shows the convergence history. Numerical simulation was performed on DEC AlphaPC workstation (processor Alpha 21164/ 533 MHz, 1GB memory).

The results of numerical computation are velocity and pressure fields in the nodes of discrete model. Figures 8 to 10 and 11 to 13 show streamlines and velocity vectors in vertical plane at 30%, 70% and 100% openings of the guard-gate. The re-circulation at the downstream end of the guard-gate may be seen.

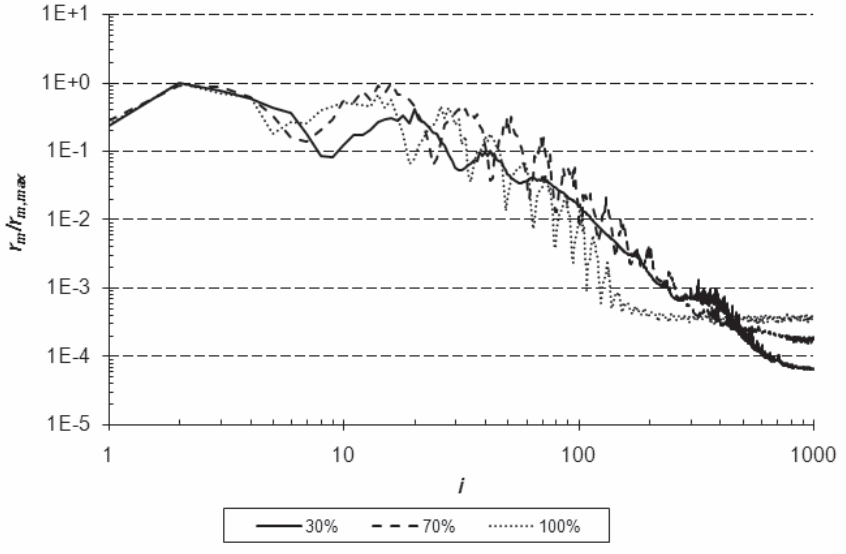

Fig. 7. *Convergence history for continuity equation residuum*

Fig. 8. *Streamlines at 30% opening of guard-gate*

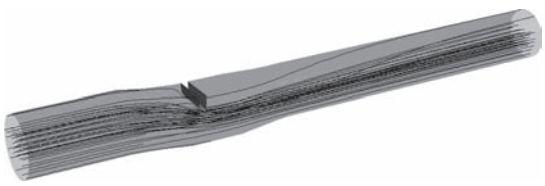

Fig. 9. *Streamlines at 70% opening of guard-gate*

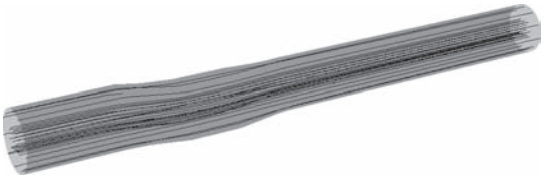

Fig. 10. *Streamlines at 100% opening of guard-gate*

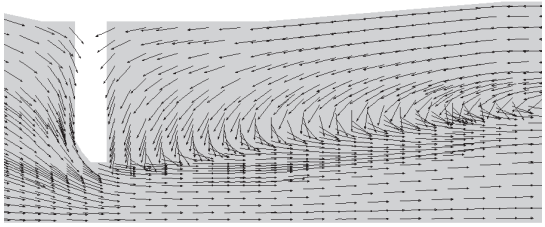

Fig. 11. *Velocity field at 30% opening of guard-gate*

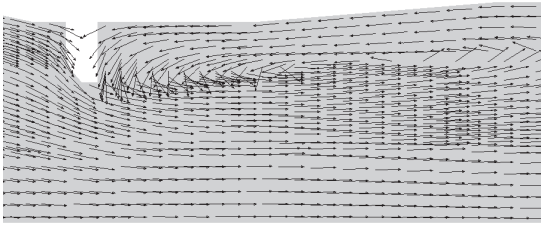

Fig. 12. *Velocity field at 70% opening of guard-gate*

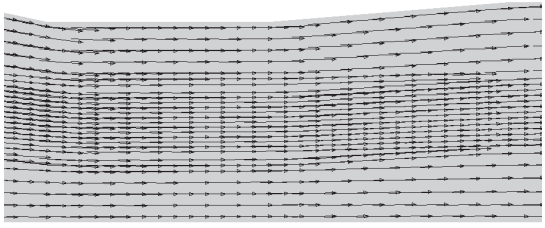

Fig. 13. *Velocity field at 100% opening of guard-gate*

2 EXPERIMENTAL APPARATUS

Experimental apparatus is installed in the High-Head Laboratory at the Institute of Hydraulic Research, Ljubljana, Figure 14. A model of Plave hydropower plant (river Soča) guard-gate was used in experiments; the scale between the model and the prototype is 1 : 20. The model apparatus includes scaled prototype gate 4 m × 5 m (width × height) with gate chamber; 105 m long, 6.5 m diameter pressure tunnel at the upstream end and 32 m long, 5.5 m diameter penstock at the downsteam end of the gate structure. The model tunnel and penstock axes are horizontal; the actual prototype penstock axis deviates 34.7° to the right and 10.2° downwards.

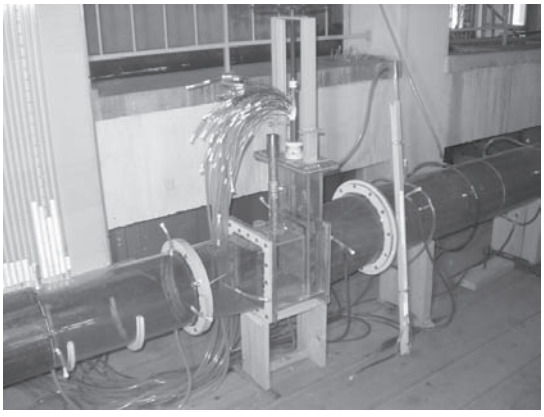

Fig. 14. *Model of the pressure tunnel; gate chamber with gate, hoist mechanism, piezometric taps and areation pipe; and penstock*

The flow rate in the model system was controlled by Thompson weir; the pressure head was adjusted by control gate valve. Pressure head measurements were performed by piezometric PVC tubes.

3 COMPARISON OF RESULTS FROM COMPUTATION AND MEASUREMENTS

Comparison of experimental and numerical results is divided into three groups. They are defined with regard to the position of pressure measuring point on the model of guard-gate, Figure 15. Upper

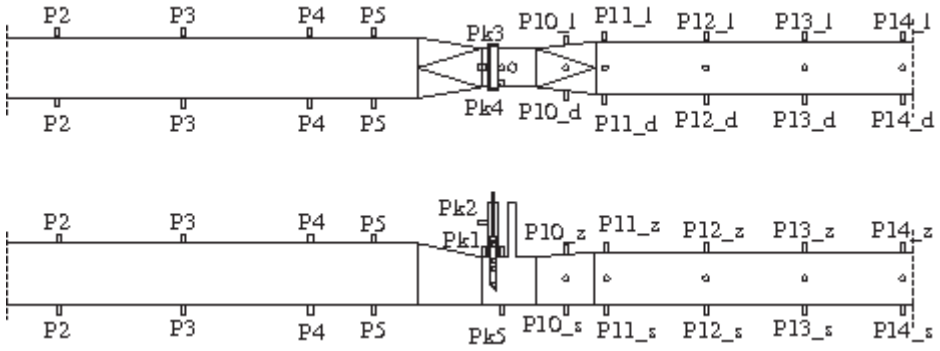

Fig. 15. *Position of piezometric taps in tunnel, gate chamber and penstock*

group is formed by experimental and numerical data which are acquired at the middle (z = 160 mm) of the upper side on the guard-gate model. Bottom group of data was acquired at the middle (z = 160 mm) of the bottom side of the model. Due to the symmetry of the guard-gate model, only the left side was considered. Measuring points with regard to:

- above: P5, PK1, PK3, P10_z, P11_z, P14_z,
- below: PK5, P10_s, P11_s,P12_s, P14_s,
- left: PQ1, PQ2, P11_l, P14_l.

Pressure measurments and corresponding numerical results are represented in Figures 16 to 18. Discrepancies of numerical results from experiment, which are given in Table 3, are normalized with regard

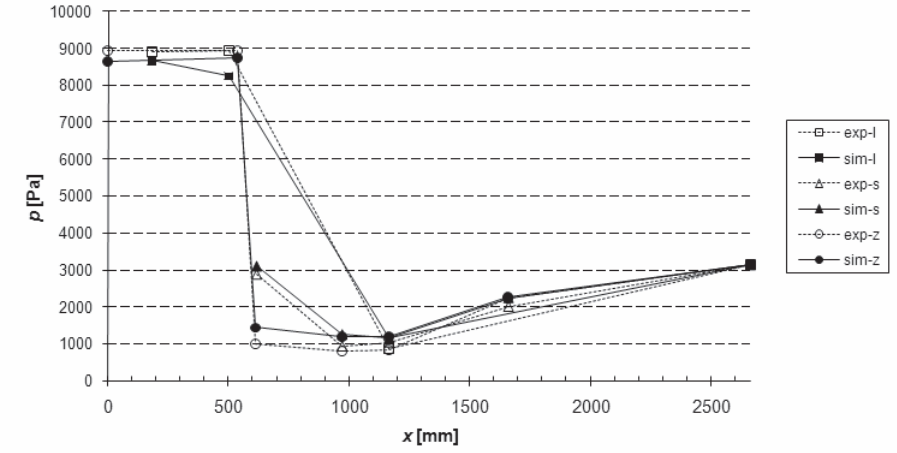

Fig. 16. *Comparison of pressures at 30% opening*

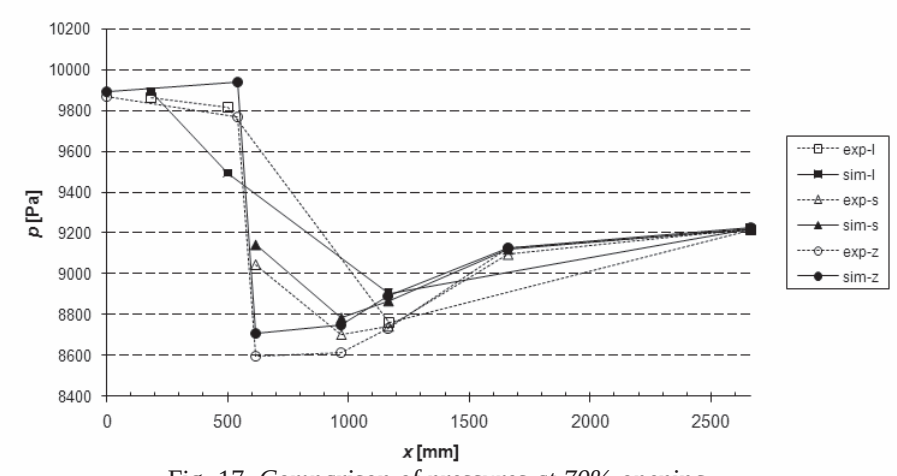

Fig. 17. *Comparison of pressures at 70% opening*

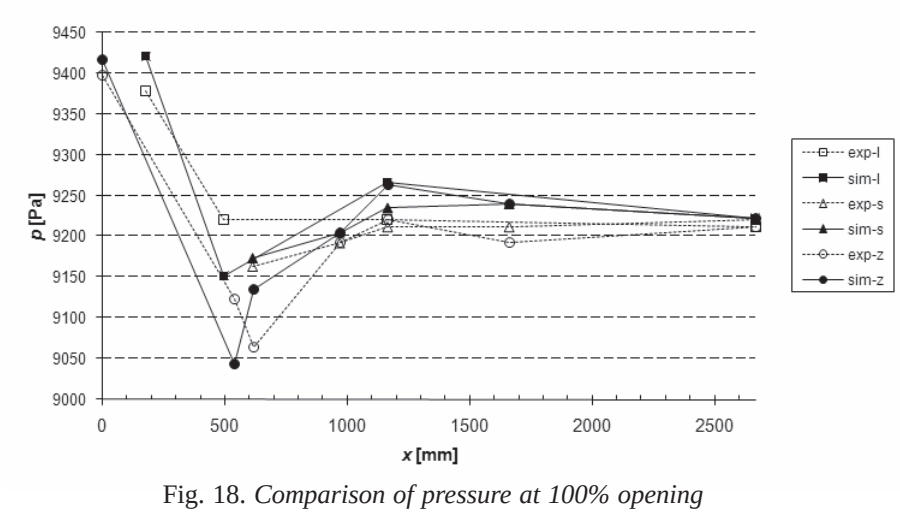

Fig. 18. *Comparison of pressure at 100% opening*

Table 3. *Descrepancies of computed pressure from measured one.*

Pa / Measuring tap	Opening [%]		
	30	70	100
P5	-3.5	1.5	5.7
PK1	-2.3	13.0	-23.8
PK3	4.9	8.9	21.2
P10_z	4.4	10.7	3.9
P11_z	4.1	12.3	12.5
P12_z	-0.1	0.3	14.4
P14_z	0.0	1.0	3.1
PK5	2.7	7.6	3.1
P10_s	3.8	6.6	3.9
P11_s	1.3	9.9	7.0
P12_s	2.7	2.1	8.5
P14_s	-0.1	0.0	0.2
PQ1	-3.2	2.5	12.8
PQ2	-8.5	-24.9	-21.1
P11_l	3.5	11.3	13.4
P14_l	0.1	0.9	3.1

to measured maximum pressure difference, which appears at particular opening of the guard-gate.

It can be observed from Figures 16 to 18 and Table 3 that the best agreement between experimental and numerical results is at 30% opening of the guard-gate. Average and maximal descrepancies at this opening reach minimum. Also the computed pressure profiles agree well with measured profiles. Comparison analysis indicates that the selected numerical model is appropriate for industrial analysis of hydraulically similar guard gates.

4 CONCLUSIONS

Analysis of gate hydraulic characteristics is essential for reliable prediction of loads acting on the guard-gate. Fluid flow characteristics were computed with the aid of the RANS k-ε turbulent model using wall functions. The system of equations is solved by the finite volume method. The results of computations were compared with the results of measurements in a guard-gate experimental apparatus. It has been found that the selected numerical model

is appropriate for industrial analysis of hydraulically similar guard gates. This would reduce a number of experimental runs in the future.

5 ACKNOWLEDGEMENT

The authors wish to thanks Litostroj Ltd. and ARRS (Slovenian Research Agency) for their generous support in the research.

6 NOMENCLATURE

C	constants of turbulence model
D	pipe diameter
$\boldsymbol{g}$	gravity acceleration
k	turbulent kinetic energy
l_{Σ}	length scale
Nc	number of cells
p	pressure
Q	volume flowrate
Re	Reynolds number
t	time
$\boldsymbol{U}$	time averaged velocity vector
U	velocity x component
V	velocity y component
W	velocity z component
x	coordinate along pipe

Greek letters:

ε	dissipation of turbulent kinetic energy
μ	laminar viscosity
μ_{ef}	effective viscosity
μ_t	turbulent viscosity
ρ	density
σ	turbulent Prandtl number

7 REFERENCES

[1] Wickert, G., Schmausser, G. *Stahlwasserbau. Theorie - Konstruktive Lösungen - Spezielle Probleme*. Berlin: Springer-Verlag, 1971.

[2] Naudascher, E. Abflussmenge und dynamische Kräfte bei Tiefschützen. *Der Bauingenieur*, 1957, 32(11), p. 428-439.

[3] Naudascher, E., Kobus, H.E., Rao, R.P.R. Hydrodynamic analysis for high head leaf gates. *Journal of the Hydraulics Division*, ASCE, 1964, 90(3), p. 155-192.

[4] Sharma, H. Air-entrainment in high head conduits. *Journal of the Hydraulics Division*, ASCE, 1976, 102(11), p. 1629-1693.

[5] Naudascher, E., Rao, R.V., Richter, A., Vargas P., Wonik, G. Prediction and control of downpull in tunnel gates. *Journal of Hydraulic Engineering*, ASCE, 1985, 112(5), p. 392-416.

[6] Naudascher, E. *Hydrodynamic forces*, IAHR Hydraulic structures manual, Vol.3, Rotterdam: A.A. Balkema, 1991.

[7] Amorin, J.C.C., de Andrade, J.L. Numerical analysis of the hydraulic downpull on vertical leaf gates. *Waterpower'99*, ASCE, Las Vegas, 1999.

[8] Patankar, S.V. *Numerical heat transfer and fluid flow*. New York: Hemisphere Publishing Corp., 1980.

[9] Ferziger, J.H., Perić, M. *Computational methods for fluid dynamics*. Berlin: Springer-Verlag, 2002.

[10] *ANSYS CFX Release 4.4 Documentation*. Harwell.

[11] Special Interest Group on "Quality and Trust in Industrial CFD". *Best parctice guidelines*. Brussels: ERCOFTAC (European Research Community On Flow, Turbulence And Combustion), 2000.

[12] Shaw, C.T. *Using computational fluid dynamics*. Englewood Cliffs: Prentice Hall Inc., 1992.

[13] Tanehill, J.C., Anderson, D.A., Pletcher, R.H. *Computational fluid mechanics and heat transfer*. Washington: Taylor & Francis, 1997.